

Improving Estuarine Transport Models using Satellite Measurements

Stefan A. Talke
Civil and Environmental Engineering Department, Portland State University
PO Box 751-CEE
Portland, OR 97207-0751
phone: (503) 725-2870 fax: (530) 725-4282 email: s.a.talke@pdx.edu

Award Number: N00014-13-1-0084

LONG-TERM GOALS

Satellite measurements of coastal and estuarine water level, water temperature, salinity, and turbidity continue to improve and now provide an opportunity to interpret coastal processes over an unprecedented range of spatial scales. Because these measurements are surface manifestations of tidal processes, river flow, and bathymetry, they can be used to obtain information about underlying physical characteristics. Improved understanding of the underlying physical processes that produce remotely-sensed surface patterns provides a means for testing and improving transport models, particularly in areas in which limited or no measurements are available.

OBJECTIVES

The overall objective of the project “Improving Estuarine Transport Models using Satellite Measurements” is to gain a better understanding of the spatial variability of surface sediment concentrations, salinity, and water temperature in estuaries, using models, in-situ data, and satellite measurements. The specific objective is to address the following questions:

- *What insights into sediment distribution, salinity, and water temperature in estuaries can be gained by collating and mining satellite images from 14+ years of MODIS satellite measurements and higher resolution LANDSAT images?*
- *Can canonical relationships for the longitudinal distribution of scalars such as salinity and turbidity be observed in satellite data under different physical conditions?*
- *Can satellite measurements of water level and scalars be used to determine system response and calibrate numerical models as a function of river flow and tidal forcing?*

APPROACH

A two-fold approach has been used since the project started in Dec. 2012. First, we are developing and refining our processing of satellite measurements, using the Columbia River estuary (CRE) as a test case due to the availability of in-situ measurements and local knowledge. Second, we are actively developing numerical modeling capabilities which we will be used to interpret results from the satellite measurement.

Following standard methods (Siegel, 2005; Palacios et al., 2009; Doxaran et al. 2009, Hu et al. 2004), we estimate turbidity and water temperature by regressing in-situ measurements against appropriate bands of surface reflectance measured by the MODerate Imaging Spectrometer (MODIS) installed on the Terra and Aqua satellites. Level 2 satellite data with atmospheric corrections are obtained from <http://ladsweb.nascom.nasa.gov/>, while in-situ data are obtained from the Center for Coastal Margin Observation and Prediction (CMOP): http://www.stccmop.org/datamart/observation_network. A total of 6 in-situ stations were used, although good quality measurements were generally available only from two locations. All satellite data are filtered for clouds, aerosols, and poor quality, and data are further binned into low, medium, and high aerosol conditions. Turbidity correlated most strongly with surface reflectance and is the focus of this report. Measurements were averaged from two to four hours centered at each MODIS pass. River flow data was obtained from the USGS, while tidal data is obtained from NOAA-CO-OPS. Ocean swell data were obtained from the National Buoy Data Center (Buoy 46029).

After calibrating the satellite data, longitudinal transects were defined along the North and South channels of the CRE so that along-estuary profiles of turbidity could be analyzed. The shape and maximum of the turbidity zone $C_b(x)$ was next approximated using the analytical model developed by Talke et al. (2009):

$$C_b(x) = A_1 \exp\{F(x)\} \quad (1)$$

$$F(x) = -A_2 s(x) + A_3 Q \exp\left(\frac{x}{L_e}\right) \quad , \quad (2)$$

where A_1 , A_2 , and A_3 are constants that depend on system characteristics such as dispersion, eddy viscosity, settling velocity, available sediment for erosion, and other parameters. The equation describes a balance between sediment flux caused by the salinity distribution $s(x)$ (or rather, processes which form the salinity structure) and freshwater flow Q . The constant L_e is the width convergence length-scale, and x is the distance from the entrance. The salinity distribution is defined by a hyperbolic tangent with ocean salinity S_o , position of maximum salinity gradient (x_c), and the length scale of the salinity gradient (x_L):

$$s(x) = 0.5S_o \left\{ 1 - \tanh\left(\frac{x - x_c}{x_L}\right) \right\} \quad (3)$$

Equation 1 was next fitted to measured turbidity transects using constrained non-linear optimization of the unknown parameters in Equations 2 and 3. Transects with mean squared errors greater than 3.5ntu were omitted, and the maximum magnitude c_{max} and x_{max} of the turbidity distribution was identified.

WORK COMPLETED

Over the past year we have successfully calibrated satellite data with in-situ turbidity and water temperature data in the Columbia River Estuary, and have identified and applied the calibration to nearly 1300 good quality images from between 1999-2013. The data are currently being evaluated statistically to determine how tidal forcing, river flow, ocean swell, and wind affect spatial patterns (see Results). A particular focus has been on comparing the South (shipping) channel with the North channel. These efforts are being led by a PhD student. A similar effort has been started on other

estuaries, focusing first on San Francisco Bay and the Ems estuary, Germany. An idealized estuarine model has been created and improved in Delft3D, and will be used to run parameter-space studies and gain insight into different riverine and tidal conditions.

In June 2013, a one-day experiment was conducted with A. Jessup’s group (UW-APL) to measure tides using airplane-based LIDAR and surface temperature using an IR camera. A total of 8 transects of ~50km length (each way) were flown between the tide gauges at Hammond and Wauna on the Columbia River. The expected resolution of the LIDAR is 0.1m rms, which should be enough to resolve the tidal range of 3m. Data is currently being corrected for airplane motions by the APL group. The expectation is that these remote measurements provide information about tidal range, tidal damping, and (through their propagation) river depth.

RESULTS

Regressions of MODIS data to *in-situ* turbidity and water temperature exhibit excellent correlation values when high-quality, low-aerosol data are used (Fig. 1). However, even images with some aerosol content show a good relationship to *in-situ* data. Hence, a large number of images are available for processing. Examples of the spatial variability of turbidity for high and low river flow are shown in Fig. 2, separated into neap and spring tides. Qualitatively, the largest turbidity is observed during spring tides and high river flow, while the lowest turbidity is measured during low river flow, low energy neap tides. Spatial variability is also evident, with shallow water regions along the fringe and at upstream intertidal areas showing elevated turbidity relative to deeper channels.

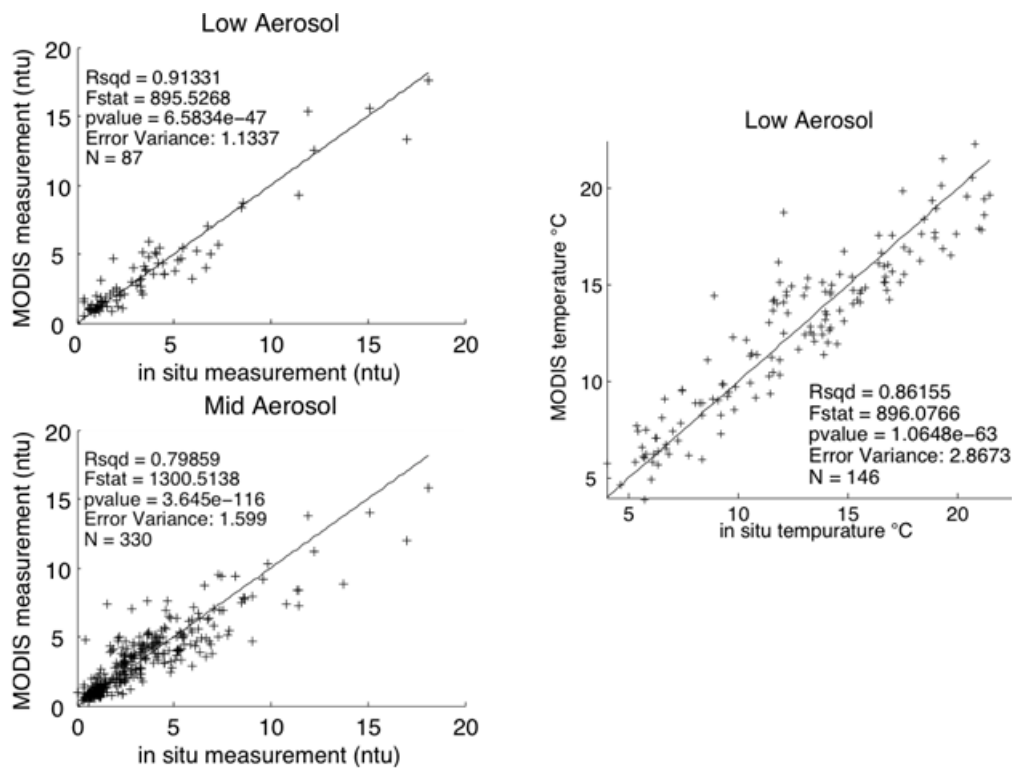


Figure 1: Regression of band 1 MODIS data against *in-situ* turbidity data (left side) and the average of band 29 and 31 against *in-situ* water temperature (right side).

The classic idea of an estuary turbidity maximum is that it occurs along the estuarine shipping channel at the toe of salinity intrusion, provided that conditions are well mixed and a tidally-averaged salinity gradient forms. To investigate this in the CRE, two transects were defined along the North and South Channels of the estuary (Fig. 2). Turbidity was derived from 250m-resolution surface reflectance, median-filtered across five adjacent pixels. Measurements containing at least 75% valid measurements (no quality flags) were used in the analysis. Between the years 2000 to 2013, a total of 1,019 and 1,265 transects were considered adequate in the South and North Channels, respectively.

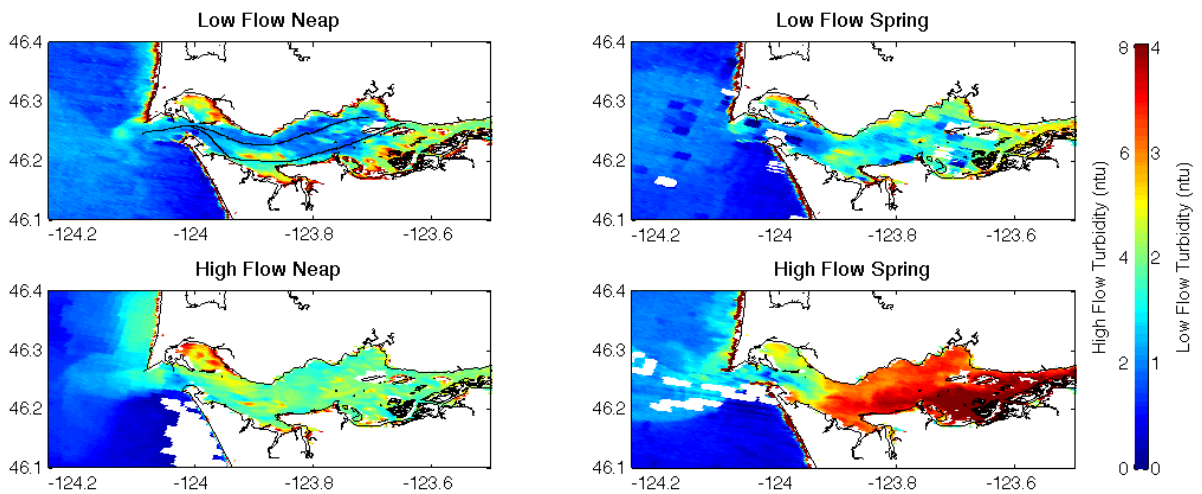


Figure 2: Examples of turbidity in the CRE for different tidal (spring, neap) and river flow conditions ($3000 \text{ m}^3/\text{s}$; $9000 \text{ m}^3/\text{s}$). The upper left image includes transect lines of the north and south channel.

Several examples of turbidity transects are shown in Fig. 3. The analytical equation well represents the shape of the turbidity zone, and filters out spurious data spikes which may occur because of pixel contamination (e.g., from nearby land pixels). Work remains to interpret the parameters in terms of physically realistic processes. Nonetheless, the fit validates a central insight of the Talke et al. 2009 model—namely, that the distribution of sediment downstream of the maximum depends on the salinity distribution (i.e., a hyperbolic tangent), and that the upstream distribution scales with river discharge. Hence, an asymmetric (non-Gaussian) profile can develop, as also observed in the data.

Evaluation of the 14 year MODIS data set demonstrates that C_{max} and the turbidity distribution around the maximum are strong functions of tidal forcing (Fig. 4). Greater tidal range leads to larger turbidity in both the North and South Channel, and increases the spatial zone of elevated turbidity, likely due to increased re-suspension and water-column mixing. Interestingly, the position of the turbidity maximum (X_{max}) is insensitive to changing tidal conditions, and varies little. The exception is neap-tidal forcing in the south channel, in which the turbidity distribution is observed to shift far upstream. We posit that this upstream maximum may result from constant sediment flux brought in by the river, which is then diluted as the estuary widens; it is also possible that turbidity moves upstream due to increased salinity intrusion during neap tides. The invariance in North Channel X_{max} indicates that this is a topographically fixed ETM, perhaps due to local bathymetric features that trap salinity and sediment, but also possibly augmented by hydrodynamic processes such as internal tidal asymmetry.

South Channel spring tides are associated with weakened salinity intrusion due to increased vertical mixing and decreasing baroclinic pressure gradients, which would drive X_{max} seaward (Jay et. al. 1990).

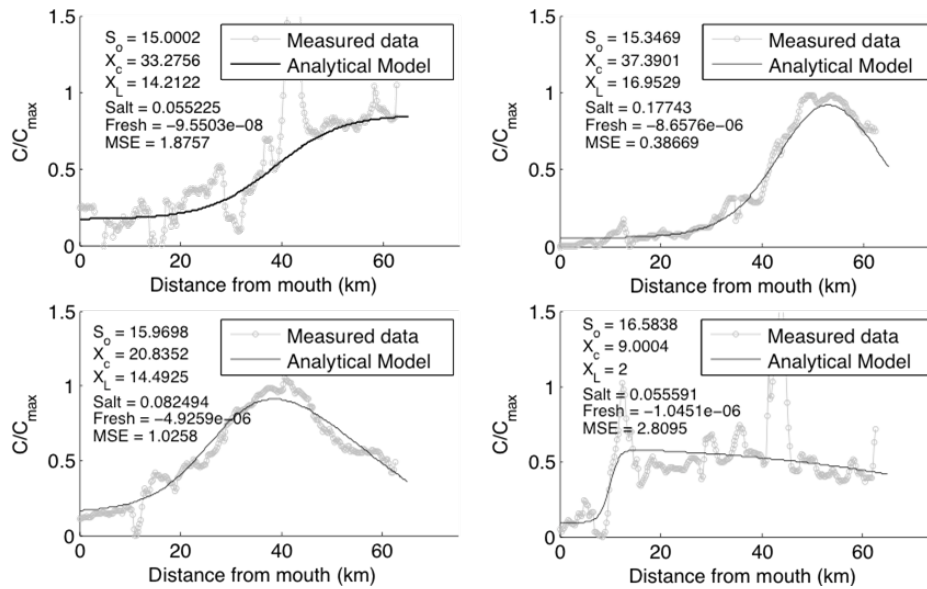


Figure 3: Transects of MODIS-based turbidity and their fit to an idealized model of turbidity, following Talke et al., 2009.

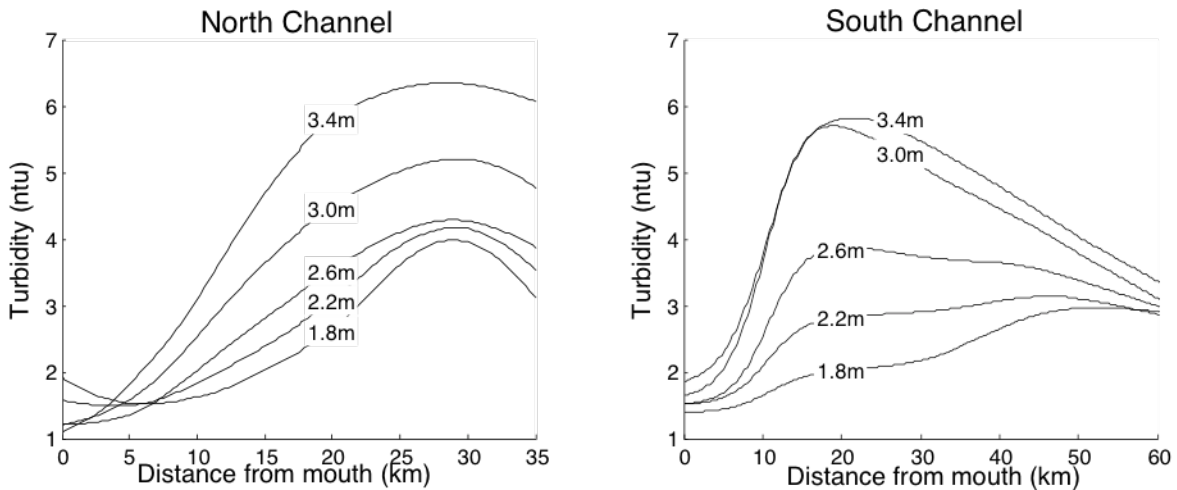


Figure 4: Comparison of turbidity in the North Channel and the South Channel for different tidal conditions.

The average turbidity and salinity fields are qualitatively correlated in the South Channel (Fig. 5). As freshwater discharge increases, the mean salinity intrusion and X_2 (the location of the 2 psu isohaline) is pushed seaward. The center of mass of the turbidity distribution follows, with sediment located more seaward (Figure 5). However, a local maximum remains apparent at $x = 15$ km; seaward of this

location, turbidity quickly decays. During low-flow conditions, a second maximum occurs around $x = 45\text{km}$, near the head of salinity intrusion. This may be evidence of a classical ETM induced by ‘well-mixed’ conditions. An interesting observation is that turbidity in the south channel displays similar patterns when responding to freshwater discharge and spring/neap cycles. During periods of downstream salinity movement, which occurs during spring tides or elevated freshwater discharge, upstream bottom flow is suppressed leading to a seaward shift in the sediment center of mass. Similarly, increased salinity intrusion brought on by neap tides and reduced river flow promotes landward flux of the salinity and turbidity fields.

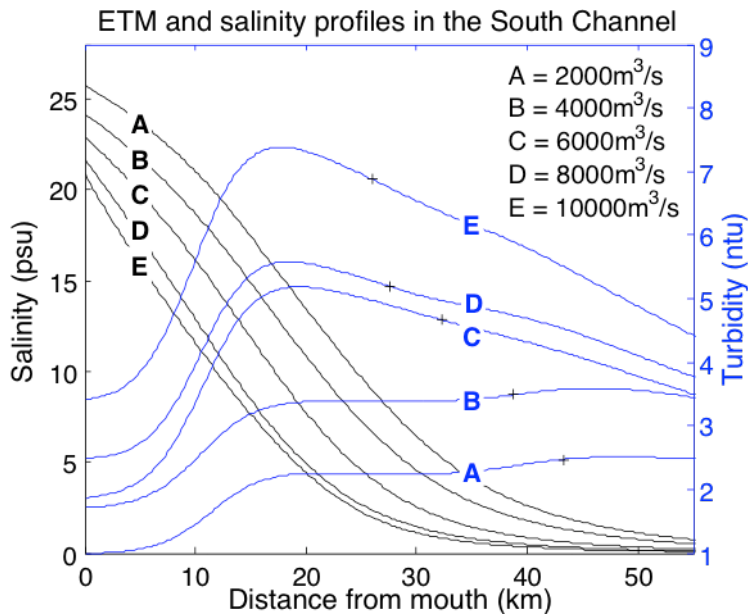


Figure 5: Comparison of satellite-derived turbidity and in-situ salinity profiles in the South Channel for different river flow conditions

Correlation maps between freshwater discharge and remotely derived turbidity (Figure 6) show that flow rate is positively correlated with turbidity throughout the estuary, particularly in the lower estuary along the North and South Channels, where C_{max} variance is greatest (Figure 4, Figure 5). Similar correlation maps for forcing at different time scales (tides, winds, etc.) significantly described a smaller portion of the turbidity variance in different regions of the system (at mid estuary for tidal range and on shallow sand flats in Cathlamet and Young’s Bay for wind).

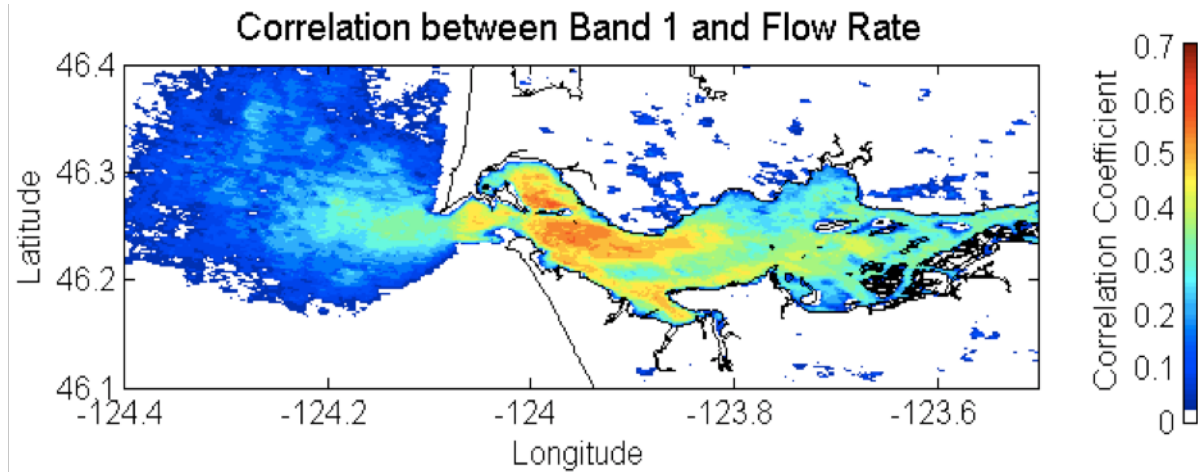


Figure 6: Correlation of river discharge with turbidity. Only statistically significant correlation is shown.

Total offshore wave energy proved also to be of significant importance to measured reflectance at the nearshore and the Mouth of the Columbia River (MCR). The influence of wave energy increases with freshwater discharge, perhaps due in part to increased suspended particulate supply (Templeton and Jay 2012) and more turbulent mixing due to wave/current interaction. Another cause may be wave breaking in the MCR during high river flow conditions, which would increase reflectance measurements. This effect remains to be investigated.

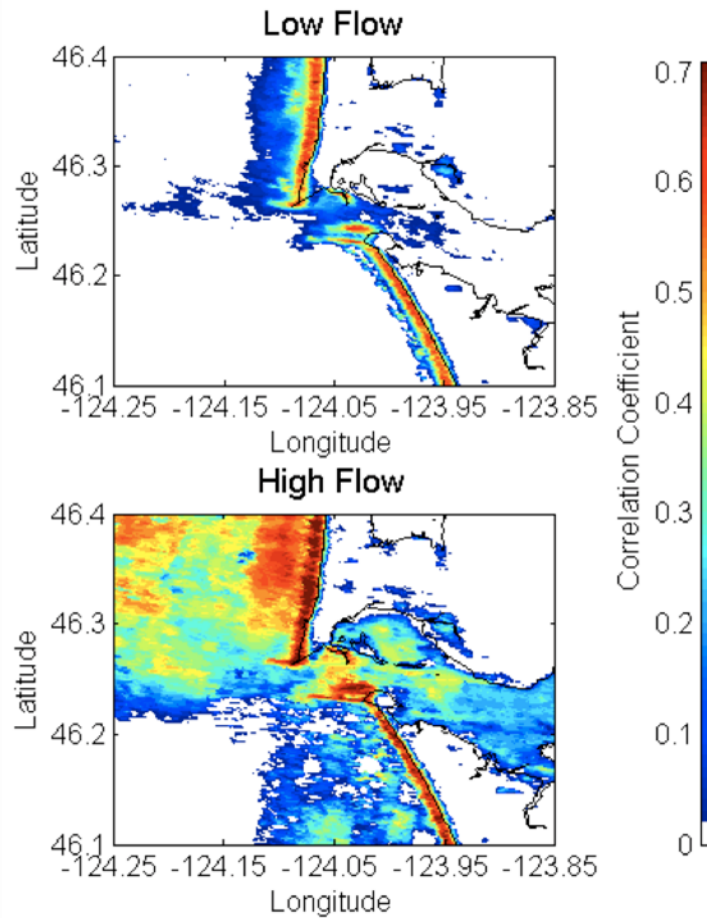


Figure 7: Correlation of wave energy with with turbidity for low $< 3000 \text{ m}^3/\text{s}$ and high ($> 9000 \text{ m}^3/\text{s}$) river flow. Only statistically significant correlation is shown.

To further investigate the development of turbidity maxima in stratified conditions, we have developed an idealized numerical model using Delft3D in which bathymetric parameters, boundary conditions, and grid characteristics can easily be altered such that a large parameter space can be investigated. An example of a turbidity maximum is shown in Fig. 8 for the case of an exponentially decreasing estuary with low flow and a constant depth. The cross section is symmetric, with a Gaussian shaped channel flanked by intertidal flats. As with field and satellite data, the shape of the turbidity maximum is asymmetric, and the position is related to the salinity gradient (not shown). Over the next year, we will modify this model to test how bathymetric features such as constrictions and depth variations trap sediment and salinity and affect the surface expression of turbidity and water temperature. Results will be used to inform limited sensitivity tests of our existing Delft 3D CRE model.

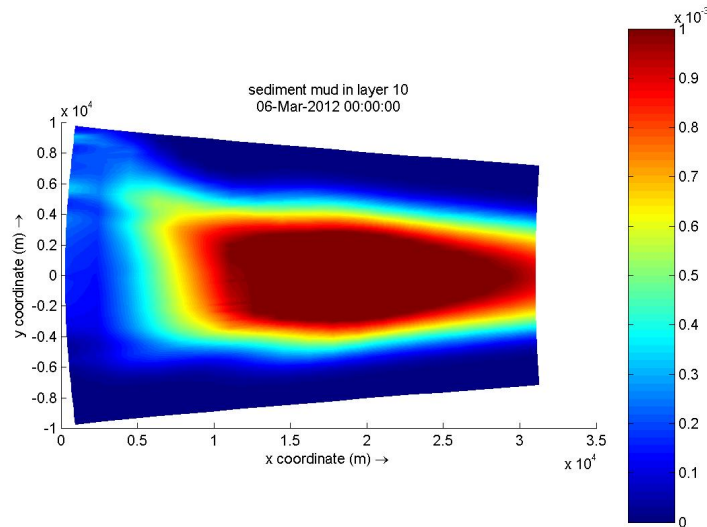


Figure 8: Example of a turbidity maximum from an idealized Delft 3D numerical model.

IMPACT/APPLICATIONS

Most previous studies of satellite data in estuaries have focused on calibration methods or have analyzed images from a few days or at most a year. This strategy yields amazing images and qualitative insights, but cannot encompass the full range of river, tidal and meteorological forcing, which shifts on daily, monthly, seasonal and longer time-scales. This study is pioneering the use of ‘satellite climatology’, in which the full satellite record is being mined to define statistically representative states that vary over the full range of forcing. This approach addresses the problem of limited temporal resolution in satellite images, which is an important issue in highly variable estuarine environments. The resulting climatology yields data that can be used to help calibrate a numerical model and constrain its parameters, and provides a snapshot of spatio-temporal variability that is not possible with *in-situ* monitoring. A particular application is to apply satellite data to locations in which limited data is available.

This project is also being used as seed-money to determine whether LIDAR can be used to estimate tides in rivers and estuaries. Since tidal data is a fundamental necessity for numerical models, remotely measuring tides could be used to help initialize and calibrate hydrodynamic and transport models in hard-to-measure areas such as shallow channels and tidal flats. Further, tides contain more information than just water level: the rate of spatial damping is related to friction and river flow, while the tidal propagation speed is a function of depth, friction, and convergence. Hence, a number of useful applications may result if this idea succeeds.

RELATED PROJECTS

The ONR-sponsored “Shallow Turbulence in Rivers and Estuaries” project is investigating large-scale eddies using *in-situ*, remotely-sensed, and modelled data. Some synergy and cross-over exists in that similar tools (the Delft3D model, satellite data) can be brought to bear on the distinct problems.

REFERENCES

- Chawla, Arun. David A. Jay, Antonio M. Baptista, Michael Wilkin. Charles Seaton. (2007). Seasonal variability and estuary-shelf interactions in circulation dynamics of a river-dominated estuary. *Estuaries and Coasts*, 31(2)p. 269-288. doi: 10.1007/s12237-007-9022-7.
- Doxaran, David. Jean-Marie Friedefond, Patric Castaing, Marcel Babin. (2009). Dynamics of the turbidity maximum zone in a macrotidal estuary (the Gironde, France): Observations from frilled and MODIS satellite data. *Estuarine, Coastal and Shelf Science*, 81p. 321-332. doi:10.1016/j.ecss.2008.11.013.
- Hu, Chuanmin. Zhiqiang Chen, Tonya D. Clayton, Peter Swarzenski, John C. Brock, Frank E. Juller Karger. (2004). Assessment of estuarine water-quality indicators using MODIS medium-resolution bands: Initial results from Tampa Bay, FL. *Remote Sensing of Environment*, 93p. 423-441. doi: 10.1016/j.res.2004.08.007.
- Jay D. A. Leffler, K. Degens, S. (2011). Long-term evolution of Columbia River tides. *J. Waterway, Port, Costal, Ocean Eng.*, 137(4)p. 182-191.
- Jay, David A., J. Dungan Smith. (1990). Circulation, density distribution and neap-spring transitions in the Columbia River Estuary. *Progress in Oceanography*, 25p. 81-112.
- Jay, David A., Philip M. Orton. Thomas Chishom. Douglas J. Wilson. Annika M. V. Fain. (2007). Partical trapping in stratified estuaries: consequences of mass conservation. *Estuaries and Coasts*, 30p.1095-1105.
- Palacios, L. Sherry. Tawnya D. Peterson., Raphael M. Kudela. (2009). Development of synthetic salinity from remote sensing for the Columbia River Plume. *Journal of Geophysical Research*, 114C00B05. doi:10.1029/2008JC004895.
- Siegel, D. A. S. Maritorena., N. B. Nelson, M. J. Behrenfeld, C. R. McClain. (2005). Colored dissolved organic matter and its influence on the satellite-based characterization of the ocean biosphere. *Geophysical Research Letters*, 32 L20605. doi:10.1029/2005GL024310.
- Talke, S.A, H.E. De Swart & H.M.Schuttelaars, 2009. Feedback between residual circulation and sediment distribution in highly turbid estuaries: an analytical model. *Continental Shelf Research*, 29(1) p. 119-135. doi:10.1016/j.csr.2007.09.002
- Templeton, J. William. David A. Jay. (2012). Lower Columbia River sand supply and removal: estimates of two sand budget components. *J. Waterway, Port, Costal, Ocean Eng.*, 139(5)p. 383-392.

PUBLICATIONS

None so far

HONORS/AWARDS/PRIZES

Outstanding Reviewer Award, *Estuaries and Coasts*, 2013 (Talke)